Heat Transfer and Entropy Generation Through Finned Tube

Prabir Kumar Nayak[a], Santosh Kumar Tripathy[b], and Dr. Ajit Kumar Senapati [c]

[a]M.Tech Scholar Thermal Engineering, Department of Mechanical Engineering, Giet University, Gunupur.
[b]Assistant Professor, Thermal Engineering, Department of Mechanical Engineering, Giet University, Gunupur.
[c]Professor and Head,Thermal Engineering, Department of Mechanical Engineering, Giet University, Gunupur..

Article History: Received: 10 January 2021; Revised: 12 February 2021; Accepted: 27 March 2021; Published online: 20 April 2021

Abstract: The study deals with the heat transfer through helical finned tube. The helical finned tube is taken in order to increase the heat transfer rate. Through the helical finned tube, the heat transfer and entropy generation are evaluated numerically on the basis of constant heat flux and constant wall temperature conditions. In case of constant wall temperature, optimised condition for fin height is obtained. At fin height of 0.002538m the heat transfer is maximum and entropy generation is neither minimum and nor maximum and it lies in between the maximum and minimum value. In case of constant heat flux conditions the entropy generation is continuously decreasing with fin height. Since, the values of heat transfer and entropy generation are calculated for helical finned tube the results obtained are fairly good, as the entropy is not increasing, using helical finned tube we can increase the heat transfer to a larger extent. The report also deals with the heat transfer through external fins, which is used in radiator. The heat transfer and entropy generation of automotive radiator have been numerically evaluated for different fin configurations (louvered, plain, and wavy fin).

Keywords*:* louvered, plain, and wavy fin

1. Introduction

This enhancement is accompanied by an increase in pressure drop. The heat transfer performance of offset strip fin is often as much as 5 times that of a plain fin surface of comparable geometry, but at the expense of higher pressure drop (Webb, 1982). For specified heat transfer and pressure drop requirements, the offset strip fin surface demands a somewhat higher frontal area compared to those with plain fin, but results in a shorter flow length and lower overall volume. An undesirable characteristic of this type of fin is that at high Reynolds numbers the friction factor remains nearly constant (because of the higher contribution of form drag), while the heat transfer performance goes down (Webb, 2000). Therefore, offset strip fins are used less frequently in very high Reynolds number applications. On the other hand, they are extensively used in air separation and other cryogenic applications where mass velocities are low and high thermal effectiveness is essential (Zdaniuk,2007).

The louvered fin geometry shown in Fig. 1(e) bears a similarity to the offset strip fin. Instead of shifting the slit strips laterally, small segments of the fin are slit and rotated 20 to 45 degrees relative to the flow direction (Jensen, 1999). The base surface of the louvered fin geometry can be of triangular or rectangular shape, and louvers can be cut in many different forms (Zdaniuk, 2008). The multi louvered fin has the highest heat transfer enhancement relative to pressure drop in comparison with most other fin types. Flow over louvered fin surfaces is similar in nature to that through the offset strip fin geometry, with boundary layer interruption and vortex shedding playing major roles. An important aspect of louvered fin performance is the degree to which the flow follows the louver (McClintock,1951; Abbassi, 2007). At low Reynolds number the flow is nearly parallel to the axial direction (duct flow), whereas at high Reynolds number the flow is in the direction of the louvers (boundary layer flow). Louvered fins are extensively used in automotive heat exchangers (Naterer, 2008).

Perforated fins shown in Fig. 1(f) are made by punching a pattern of spaced holes in the fin material before it is folded to form the flow channels (Demirel, 1999). The channels may be triangular or rectangular in shape with either round or rectangular perforations. While this geometry, with boundary layer interruptions, is a definite improvement over plain fins, its performance is generally poorer than that of a good offset strip fin (Ahmet,2003). Furthermore, the perforated fin represents a wasteful way of making an enhanced surface, since the material removed in creating the perforations is thrown out as scrap. Perforated fins are now used only in limited number of applications such as turbulators in oil coolers (Oliet, 2007).

In a pin fin exchanger, a large number of small pins are sandwiched between plates in either an inline or staggered arrangement. Pins may have a round, an elliptical, (Peyghambarh, 2011) or a rectangular cross section. These types of finned surfaces are not widely used due to low compactness and high cost per unit surface area compared to multi louvered or offset strip fins. (Leong,2010) Due to vortex shedding behind the pins, noise and flow-induced vibration are produced, which are generally not acceptable in most heat exchanger applications. The potential application of pin fin surfaces is at low flow velocities (Re < 500), where pressure drop is negligible. Pin fins are used as electronic cooling devices with free-convection flow on the pin fin side. Extended or finned surfaces are widely used in compact heat exchanger to enhance the heat transfer and reduce the size. Common among these are automobile radiators, charge air coolers, automobile air-conditioning evaporators and condensers to meet the demand for saving energy and resources. In these applications, the heat transfer is normally limited by

the thermal resistance on the air side of the heat exchangers. Therefore, various augmented surfaces have been developed to improve air side heat transfer performance. Typical fin geometries are plain fins, wavy fins, offset strip fins, perforated fins and multi-louvered fins, which, besides increasing the surface area density of the exchanger, also improve the convection heat transfer coefficients. Of these, wavy fins are particularly attractive for their simplicity of manufacture and potentials for enhanced thermal-hydraulic performance. The air side thermal hydraulic performance of wavy fin and round tube heat exchangers have been studied by many researchers. However, the study of wavy fin and flat tube heat exchanger is very limited (Chang, 1997)

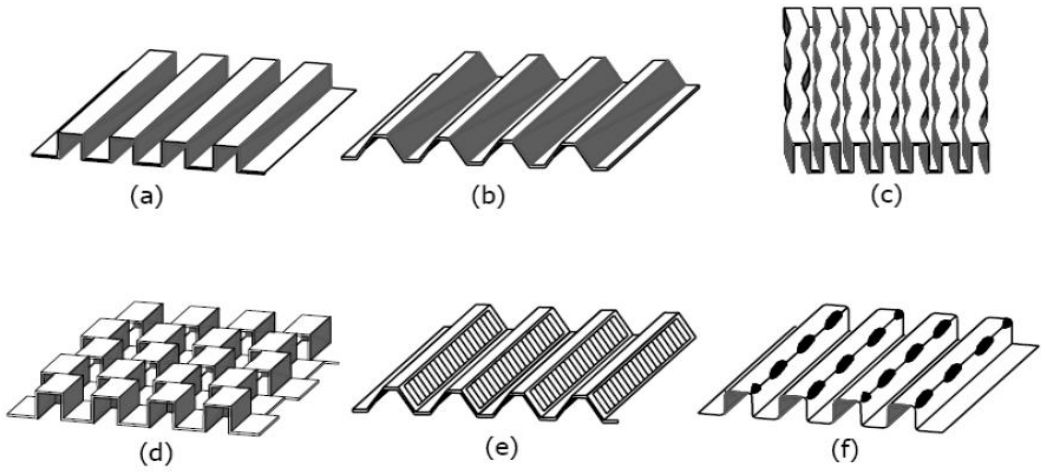

Figure: 1. Types Of Plate fin Surfaces (A) Plain Rectangular (B) Plain trapezoidal (c) Wavy (D) Off set strep pin (E) Louvered (F) Perorated

1.1. Entropy Generation

Entropy is a measure of molecular disorder or randomness of a system, and the second law states that entropy can be created but it cannot be destroyed. The increase of entropy principle is expressed as

Entropy change = Entropy transfer + Entropy generation

$\Delta S_{system} = S_{transfer} + S_{gen}$

The entropy change of a system or its surroundings can be negative; but entropy generation can not.

$S_{gen} = 0$ for reversible process

$S_{gen} > 0$ for irreversible process

$S_{gen} < 0$ for impossible process

2. Mathematical Modelling

2.1Physical geometry:

2.1.1 For internally finned tube

One contemporary enhancement geometry is the helical fin shown in figure which is described by several geometric variables.Figure also provides a pictorial description of these variables, which include: the fin height (e), the fin pitch (p), the helix angle (α), number of starts (N_s), and included angle (β). The fin height is the distance measured from the internal wall of the tube to the top of the fin. The fin pitch is the distance between the centers of two fins measured in the axial direction. The helix angle is the angle the fin forms with the tube axis. The number of starts refers to how many fins one can count around the circumference of the tube. Finally, the angle at which the sides of the fin meet is called the included angle

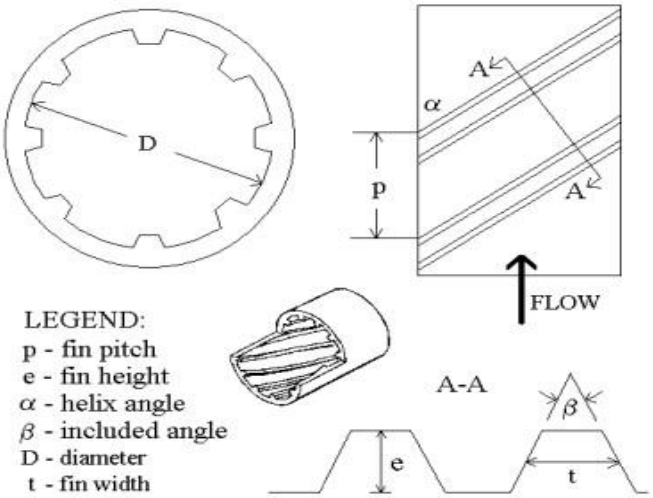

Figure.2 Legend

2.1.2 Assumptions:

- Steady state
- Fully developed flow
- Fluid flow only inside the tube
- The potential and kinetic energy changes are negligible.
- The radiation heat transfer from tubes is negligible

2.1.3 Equations:

The following equations are used to correlate the numerical data shown:

The following correlation are used

$$f = 0.128Re^{-0.305}\, Ns^{0.235}\, (e/D)^{0.319}\alpha^{0.397} \quad (1)$$

and

$$j = 0.029Re^{-0.347}\, Ns^{0.253}\, (e/D)^{0.0877}\alpha^{0.362} \quad (2)$$

From the above correlation we can get

$$Nu = 0.029Re^{0.653}\, Ns^{0.253}\, (e/D)^{0.0877}\alpha^{0.362}Pr^{(1/3)} \quad (3)$$

Heat transfer coefficient

$$h = \frac{Nu \times k}{D} \quad (4)$$

Perimeter of the pipe

$$p = 2 \times \frac{e}{\cos\beta} + b \quad (5)$$

Pressure drop in the tube

$$dP = \frac{f \times L \times V^2 \times \rho}{2 \times D} \quad (6)$$

Surface area of the helically finned tube

$$A_s = \left(\pi D - N_s \frac{a}{\cos\alpha}\right) L + N_s p \frac{L}{\cos\alpha} \tag{7}$$

Cross sectional area of the helically finned tube

$$A_c = \frac{\pi}{4} D^2 - \frac{N_s}{2}(a+b)\frac{e}{\cos\alpha} \tag{8}$$

Mass flow rate, $$\dot{m} = \rho A_c V \tag{9}$$

There are two conditions for the tube

(1) Constant wall temperature of the tube

Heat transfer rate from the tube

$$Q = UA_s(\Delta T_m) \tag{10}$$

$$= mC_p\left[(T_b)_{exit} - (T_b)_{inlet}\right] \tag{11}$$

Logarithmic mean temperature difference

$$\Delta T_m = \frac{(T_w - T_a) - (T_w - T_e)}{\ell n\left(\frac{T_w - T_a}{T_w - T_e}\right)} \tag{12}$$

From above we get,

$$T_e = T_w - \frac{T_w - T_a}{e^{\left(\frac{UA_s}{mC_p}\right)}} \tag{13}$$

Pressure at inlet side of the tube

$$P_1 = P_2 + dP \tag{14}$$

Entropy generation

$$S_{gen} = m\left[C_p \ell n \frac{T_e}{T_a} - R\ell n \frac{P_2}{P_1}\right] - \frac{Q}{T_w} \tag{15}$$

(2) Constant heat flux of the tube

$$Q = A_s h(T_w - T_e) = mC_p(T_e - T_a) \tag{16}$$

Exit temperature

$$T_e = \frac{Q}{(mC_p)} + T_a \tag{17}$$

Entropy generation

$$S_{gen} = m\left[C_p \ell n\left(\frac{T_e}{T_a}\right) - R\ell n\left(\frac{P_2}{P_1}\right)\right] - p_w hL \frac{(T_w - T_e)}{(T_e - T_a)} \ell n\left(\frac{T_e}{T_a}\right) \tag{18}$$

2.1.4 Air side calculation

Initially, air side calculations were performed to determine air heat capacity, air heat transfer coefficient, fin efficiency and total surface temperature effectiveness. These data were needed to calculate heat exchanger effectiveness, NTU number and overall heat transfer coefficient for the base fluid side calculation. The mathematical formulations are shown below.

Air heat capacity rate, C_a can be expressed as [16]

$$C_a = W_a C_{p,a} \tag{19}$$

Core mass velocity of air is expressed as [16]

$$G_a = \frac{W_a}{A_{fr}\sigma_a} \tag{20}$$

Heat transfer coefficient, h_a can be expressed as [16]

$$h_a = \frac{j_a G_a C_{p,a}}{Pr_a^{2/3}} \tag{21}$$

Correlation for the Colburn j factor

$$j_a = \frac{0.174}{Re_a^{0.383}} \quad \text{(For plate fin [16])} \tag{22}$$

$$j_a = 0.26712\,Re_a^{-0.1944} \times \left(\frac{L_a}{90}\right)^{0.257} \times \left(\frac{F_p}{L_p}\right)^{-0.5177} \times \left(\frac{F_h}{L_p}\right)^{-1.9045} \times \left(\frac{L_h}{L_p}\right)^{1.7159} \times \left(\frac{L_d}{L_p}\right)^{-0.2147} \times \left(\frac{t}{L_p}\right)^{-0.05}$$

(For Louvered fin[17] (23)

$$j_a = 0.0836\,Re_a^{-0.2309} \times \left(\frac{F_p}{F_h}\right)^{0.1284} \times \left(\frac{F_p}{2A}\right)^{-0.153} \times \left(\frac{L_d}{L}\right)^{-0.326}$$

(For Wavy fin) (24)

$$f_a = 1.16\,Re_a^{-0.309} \times \left(\frac{F_p}{F_h}\right)^{0.3707} \times \left(\frac{F_p}{2A}\right)^{-0.25} \times \left(\frac{L_d}{L}\right)^{-0.1152}$$

Reynolds number expression for plate fin and louvered fin is expressed as F_h

$$Re_a = \frac{G_a D_{ha}}{\mu_a} \quad \text{(Plate fin [16])} \tag{25}$$

$$Re_a = \frac{\rho_a u_a L_p}{\mu_a} \quad \text{(Louvered fin [17])} \tag{26}$$

Where air velocity is given by,

$$u_a = \frac{G_a}{\rho_a} \tag{27}$$

Plate fin efficiency ,η_f can be expressed as [16]

$$\eta = \frac{\tanh m\ell}{m\ell} \tag{28}$$

$$m = \sqrt{\frac{2h_a}{kt}} \quad (29)$$

Where,

Total surface temperature effectiveness, can be expressed as [16]

$$\eta_0 = 1 - \frac{A_f}{A}\left(1 - \eta_f\right) \quad (30)$$

Entropy generation on air side :

$$dS_a = W_a \times C_{p,a} \times \ell n\left(\frac{T_{out}}{T_{in}}\right) - W_a \times R_a \times \ell n\left(\frac{P_{out}}{P_{in}}\right) \quad (31)$$

2.1.3 Coolant side calculation

The parameters needed for base fluid side calculation are base fluid heat transfer coefficient, base fluid heat capacity rate.

Heat transfer coefficient can be expressed as:

$$h_{bf} = \frac{N_{u,bf} \times k_{bf}}{D_{h,bf}} \quad (32)$$

$$(Nu)_{bf} = 0.021\ (Re_{bf})^{0.8}\ (Pr_{bf})^{0.5} \quad (33)$$

Reynolds no. expression for base fluid

$$R_{ef} = \frac{G_f \times D_{h,bf}}{\mu_{bf}} \quad (34)$$

Prandtl number expression for base fluid is

$$(Pr)_{bf} = \frac{\mu \times C_{p,bf}}{k_{bf}} \quad (35)$$

Pressure drop can be expressed as:

$$(dP)_{bf} = \frac{G_{bf}^2 \times f \times H}{2 \times \rho \times \frac{D_{h,bf}}{4}} \quad (36)$$

Where , the friction factor correlation of base fluid is given by

$$f = 0.3164\ Re^{-0.25} \quad (37)$$

Entropy generation on fluid side:

$$(ds)_f = w_{bf} \times C_{p,bf} \times \ell n\left(\frac{T_{out}}{T_{in}}\right) + \frac{w_f \times D_{p,bf}}{\rho \times T} \quad (38)$$

Where

$$T = \frac{(T)_{out} + (T)_{in}}{2} \quad (39)$$

2.1.4 Performance calculation:

Overall heat transfer coefficient, based on air side can be expressed as below where wall resistance and fouling factors are neglected.

$$\frac{1}{U_a} = \frac{1}{h_a} + \frac{1}{h_{bf}} \tag{40}$$

Number of heat transfer unit is expressed as

$$NTU = \frac{U_a A_{fr,a}}{C_a} \tag{41}$$

Heat exchanger effectiveness for cross-flow unmixed fluid can be expressed as [16],

$$\varepsilon = 1 - e^{\left[\frac{NTU^{0.22}}{C^*} e^{\left(-C^* NTU^{0.78} - 1\right)}\right]} \tag{42}$$

Where, $$C^* = \frac{C_{min}}{C_{max}} \tag{43}$$

Total heat transfer rate can be expressed as:

$$Q = \varepsilon C_{min}(T_{bf,\,in} - T_{a,\,in}) \tag{44}$$

Total entropy generation is given by:

$$S_{gen} = dS_a + dS_{bf} \tag{45}$$

Validation:

The result of this analysis is same as theoretically and data with an error of less than 10% experimentally.

2.2Input parameters:

The input parameter of internally finned tube is given in the table 1 and for the radiator in table 2 to 6. The radiator which is considered here is mounted on the present turbo-charged diesel engine of type TBD 232V-12 is cross flow compact exchanger with unmixed fluids in (Fig.2). Radiator consists of 644 tubes make of brass and 346 continuous fins made of Aluminum alloy whose thermal conductivity is 177W/m K [16]. The common geometrical factors and operating conditions are described in the Tables 2 and 3. Additional geometric parameters for louvered fin are given in Table 4. Properties of base fluid and air are given in Table 5. Properties of wavy are given in Table 6.

Table 1: Parameters for the internally finned tube

Input Parameter	**Values**
D(m)	0.01564
e(m)	0.00038 to0.0055
Ns	10
α(˚)	25
E=e/D	0.0243
k(w/m-k)	0.026
v(m/s)	10
Re	10000
β(˚)	41
Pr	0.70
a(m)	0.00048
b(m)	0.0002
L(m)	1

Ta(K)	298
Tw(K)	353
Cp(J/kg-k)	1005
R(J/kg-k)	287
g(m/s^2)	9.81
P_2=P(N/m^2)	101325
ρ(kg/m^3)	1.2

Table 2: Fluid parameters and Normal Operating conditions

S.NO.	Description	Air	Coolant
1	Fluid mass rate	10-20kg/s	4-6kg/s
2	Fluid inlet temperature	10-50^{0}C	80-100^{0}C
3	Core Width	0.6m	
4	Core height	0.5m	
5	Core depth	0.4m	

Table 3: Surface core geometry of flat tubes, continuous fins.

S.NO.	Description	Air side	Coolant side
1	Fin pitch	4.46fin/cm	
2	Fin metal thickness	0.01cm	
3	Hydraulic diameter D_h	0.351cm	0.373cm
4	Min free flow area/frontal area σ	0.780	0.129
5	Total heat transfer area/total volume α	886 m^2/m^3	138 m^2/m^3
6	Fin area/Total area β	0.845	

Table 4: Thermal physical properties of Base fluid (80%water-20%etylene glycol) and Air

S.NO.	Thermal physical properties	Base fluid	Air
1	Density(kg/m^3)	1008	1.1614
2	Specific heat (J/kg K)	4020	1007
3	Viscosity(N-s/m^2)	0.0019	0.00001846
4	Conductivity(W/m K)	0.58	

Table 5: Specification of multi-louvered fin parameters

1	L_a	28°
2	F_p	2 mm
3	L_p	1.2 mm

4	F_h	8 mm
5	L_h	6.5 mm
6	L_d	36.6 mm

Table 6: Specification of wavy fin parameters

1	F_p	2 mm
2	2A	1.5 mm
3	F_h	8 mm
4	L	10.8 mm
5	L_d	65 mm

2.3 Result and Discussion:

A computer software programme in MATLAB has been developed to determine all the parameters i.e. heat transfer rate, entropy generation, pressure drop etc. for both internally finned tube and automotive radiator.

2.4.Results for internally finned tube:

2.4.1For constant wall temperature:

2.4.1(a) Variation of heat transfer with respect to fin height

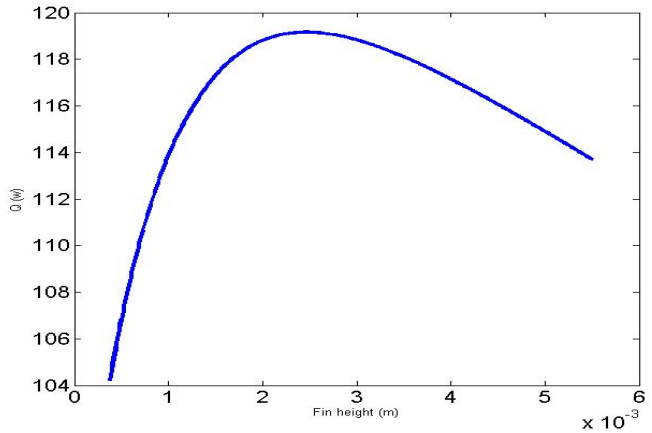

Figure 2. Heat transfer vs fin height

In the Fig. 2, initially heat transfer increases after some time it will be maximum and then decreases.

The maximum heat transfer = 119.2 Watt

The fin height at maximum heat transfer =0.00253m

2.4.1(b) Variation of entropy generation with respect to fin height

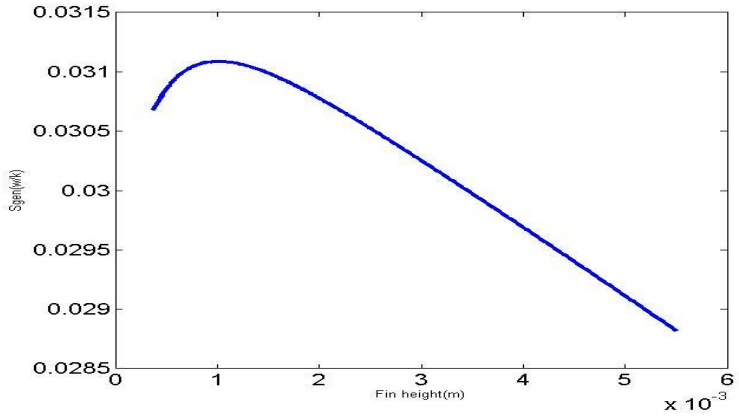

Figure 3: Entropy generation vs fin height

In this Fig. 3 entropy generation increases initially it will be maximum after some time and then decreases. Maximum entropy generation =0.0311 W/K& Fin height at maximum entropy generation =0.0011m

2.4.1(c) Variation of pressure drop with respect to fin height

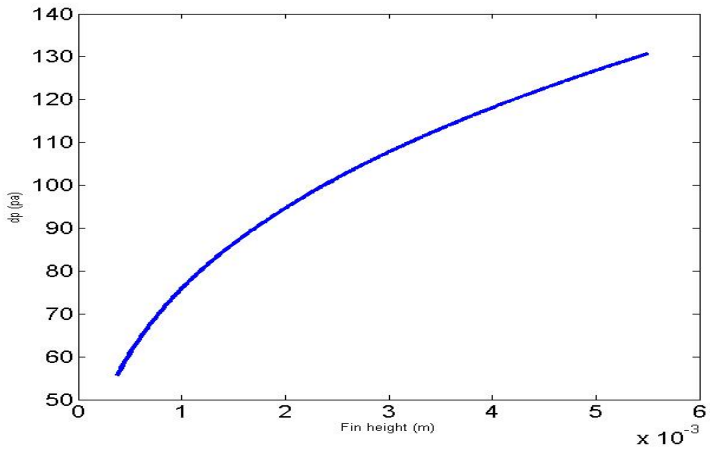

Figure 4. Pressure drop vs fin height

The pressure drop increases consistently with fin height because if fin height increases it restricts the flow due to which pressure drop increases. If fin height is more, then considerable pressure drop will be there.

2.4.1(d) Variation of friction factor with respect to fin height

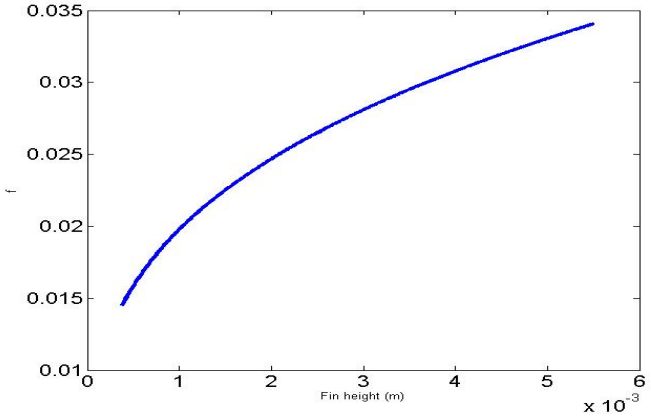

Figure 5: Friction factor vs fin height

The curve of friction factor is analogous to the pressure drop .It is also increasing consistently with fin height. It is happening just because of fin height, if the fin height is more then it behaves like a rough surface. If the surface is rough then the friction will be more.

2.4.1(e) Variation of temperature drop with respect to fin height

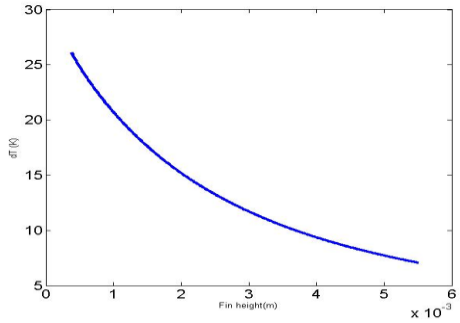

Figure 6: Logarithmic mean temperature difference vs fin height

If the fin height increases the Logarithmic mean temperature difference decreases. The nature of graph is logarithmic. Both Logarithmic mean temperature difference and fin height is inversely proportional to each other.

2.4.1(f) Optimised graph between heat transfer and entropy generation with respect to fin height

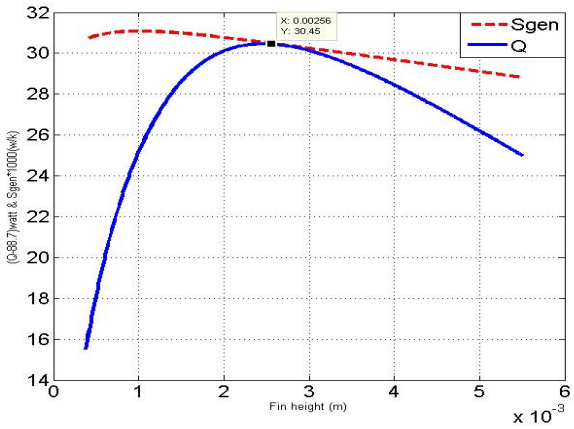

Figure 7. Optimised graph between heat transfer, entropy generation and fin height

Here both the graph initially increases and then attain maximum value and then decreases with fin height. But both heat transfer and entropy generation is maximum at different fin height. Here optimisation is done on the basis of maximum heat transfer.

Maximum heat transfer =119.2watt at fin height =0.0053m

Maximum entropy generation =0.0311 W/K at fin height =0.0011m

Optimised value

At fin height =0.00253m

Maximum heat transfer =119.2 Watt

Entropy generation =0.00305 W/K

2.4.2. For constant heat flux condition:

2.4.2(a) Variation of entropy generation with respect to fin height

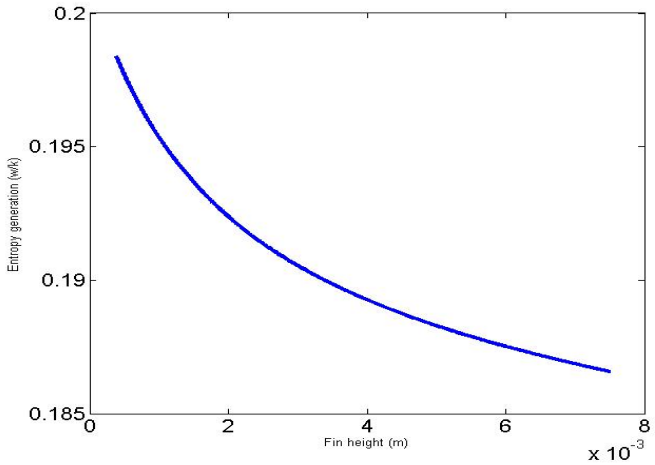

Figure 8. Entropy generation vs fin height

Entropy generation is continuously decreasing with fin height. The curve of entropy generation is logarithmic in nature. The value of entropy generation in constant heat condition is more as compared to constant wall temperature at corresponding fin height.

2.4.2(b) Variation of pressure drop with respect to fin height

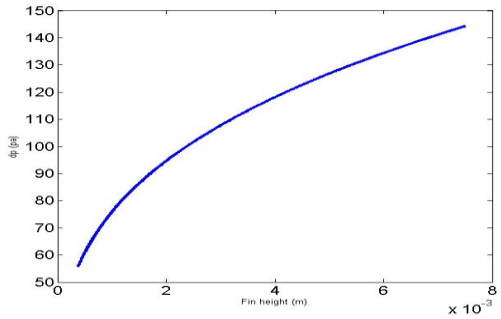

Figure 9: Pressure drop vs fin height

The pressure drop increases consistently with fin height because if fin height increases it restricts the flow due to which pressure drop increases. If fin height is more, then considerable pressure drop will be there.

2.4.2(c) Variation of friction factor with respect to fin height

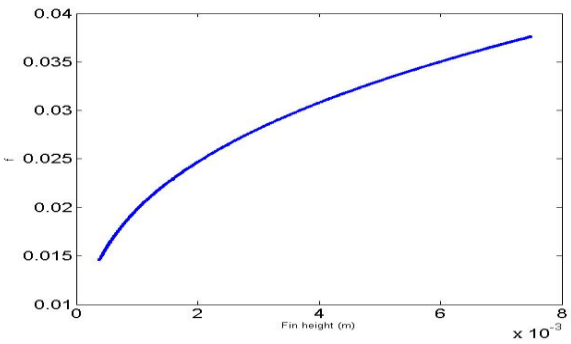

Figure 10. Friction factor vs fin height

The curve of friction factor is analogous to the pressure drop .It is also increasing consistently with fin height. It is happening just because of fin height, if the fin height is more then it behaves like a rough surface. If the surface is rough then the friction will be more.

2.4.2(d)Variation of temperature drop with respect to fin height

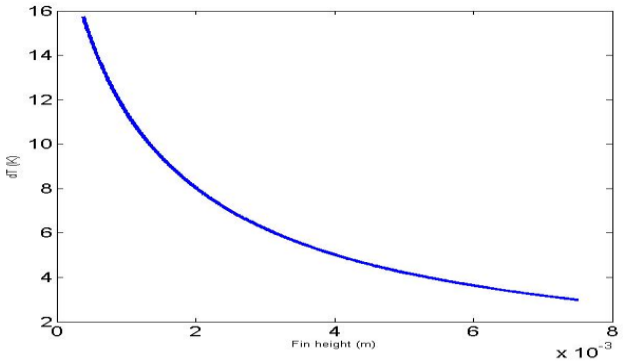

Figure 11. Temperature difference vs fin height

If the fin height increases the temperature difference decreases. The nature of graph is logarithmic. Both temperature difference and fin height is inversely proportional to each other.

2.5. Results for Plate fin Radiator:

2.5.1 Influence of varying inlet air mass flow rate:

The variation of cooling capacity and effectiveness with air mass flow rate from 10 to 20 kg/s is shown in Fig. keeping constant average values for other input data(m_c=5kg/s, T_{ai}=30°C, T_{nfi}=90°C). It has been found that with increase in mass flow rate of air, cooling capacity goes on increasing because of increasing heat transfer coefficient and the effectiveness for cooling is goes on decreasing. And in Fig.2.12 entropy generation increases with air mass flow rate.

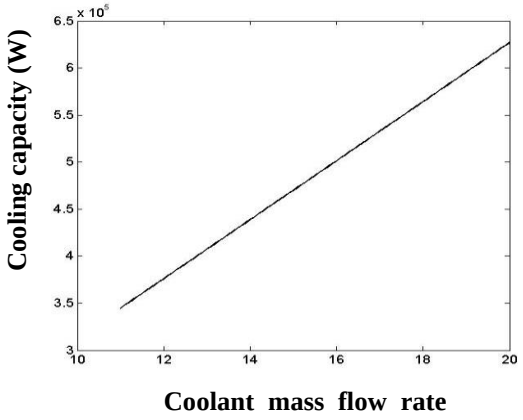

Figure 12: Effect of mass flow rate of air on cooling capacity

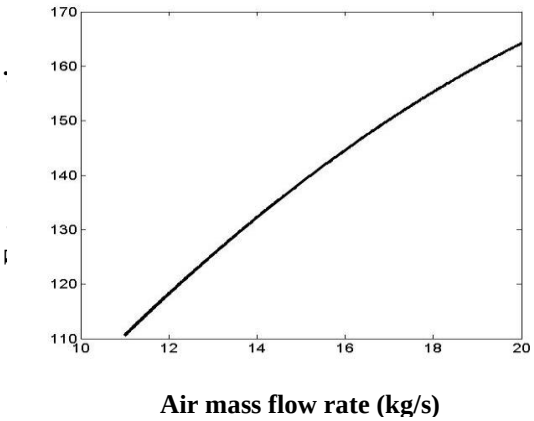

Figure 13: Effect of mass flow rate of air on entropy generation

2.5.2 Influence of varying coolant mass flow rate:

Result (Fig.14) shows that with the variation of coolant mass flow rate, pressure drop increases because pressure drop is directly proportional to the velocity of the coolant, and velocity is directly proportional to the mass flow rate of the coolant. And in Fig.15 entropy generation increases with coolant mass flow rate.

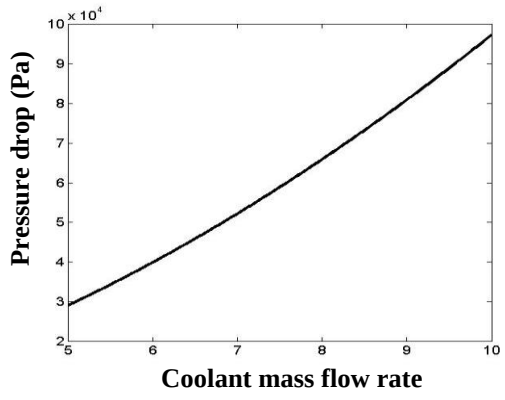

Figure 14: Effect of mass flow rate of coolant on pressure drop

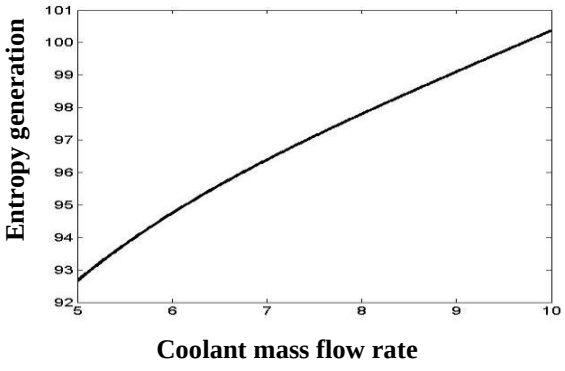

Figure 15: Effect of mass flow rate of coolant on entropy generation

2.5.3 Influence of varying inlet air temperature:

The variation of cooling capacity and effectiveness with air inlet temperature is shown in Fig.2.15 for (m_c=5kg/s, m_a=10kg/s, T_{nfi}=90°C). As expected the heat transfer rate clearly decreases with air inlet temperature rise, as the cooling temperature difference is being reduced.

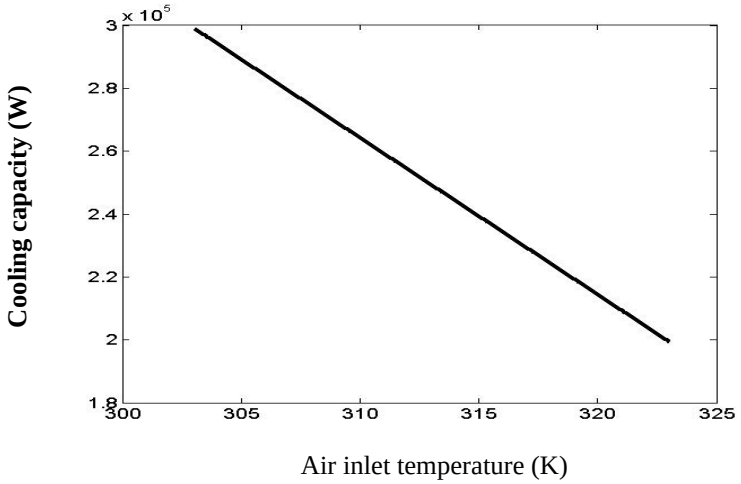

Figure 16: Effect of air inlet temperature on cooling capacity

2.5.4 Influence of varying coolant inlet temperature:

The variation of cooling capacity with coolant inlet temperature is shown in Fig.17 for (m_c=5kg/s, m_a=10kg/s, T_{ai}=30^0C). As expected the heat transfer rate increases with coolant inlet temperature rise due to increment in the cooling temperature difference.

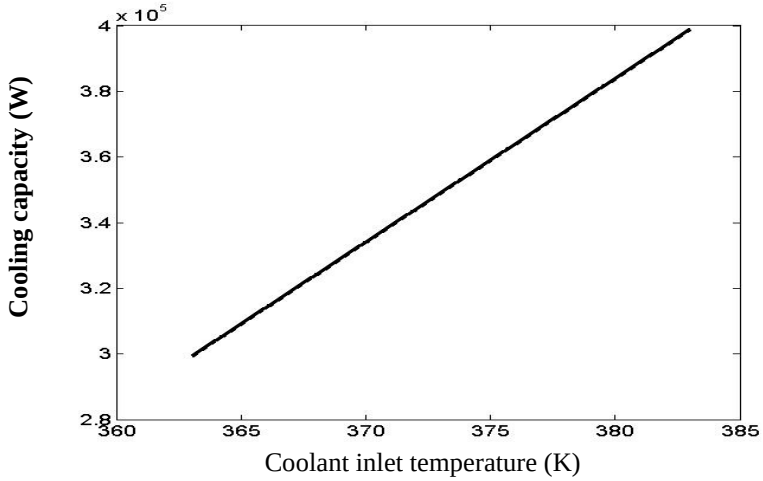

Figure 17: Effect of coolant inlet temperature on cooling capacity

2.6. Results for louvered fin Radiator:

For enhancing heat transfer rate, louvered fin geometry has been used. As shown in Figs.18-22, the parametric variations are similar to plate fin. As discussed earlier for the plate fin geometry that with the variation of inlet air mass flow rate, cooling capacity increases while effectiveness decreases, on comparing its performance with plate fin geometry about 8% enhancement in the cooling capacity is observed (Fig. 18). In the similar manner, cooling capacity, effectiveness, pressure drop increases with increase in coolant mass flow rate keeping other factors as a constant (Fig. 19). On increasing inlet air temperature, the reduction in cooling capacity of radiator is observed (Fig. 20) while the cooling capacity increases with the increase in coolant inlet temperature (Fig. 21). And on increasing in mass flow rate of coolant, the entropy generation increases (Fig. 22).

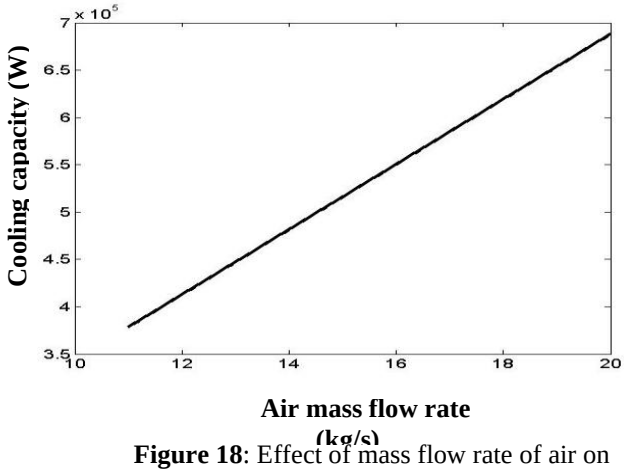

Figure 18: Effect of mass flow rate of air on cooling capacity

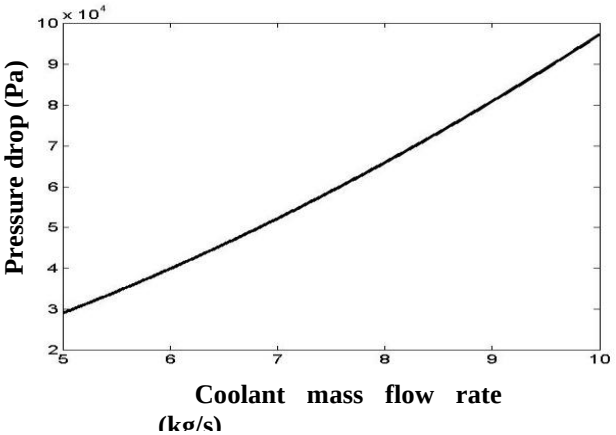

Figure 19: Effect of mass flow rate of coolant on pressure drop

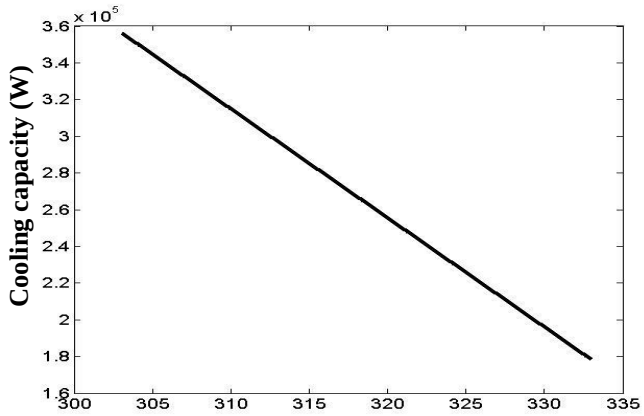

Figure 20: Effect of air inlet temperature on cooling capacity

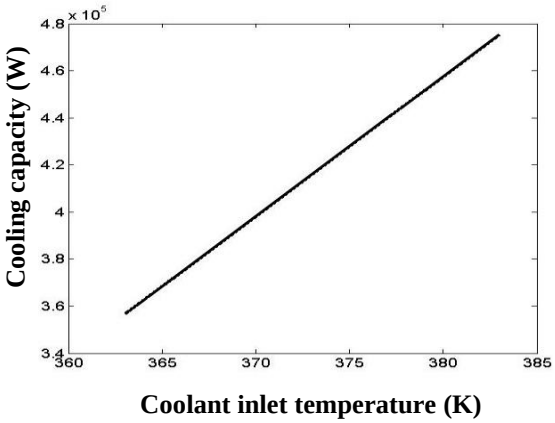

Figure 21: Effect of coolant inlet temperature on cooling capacity

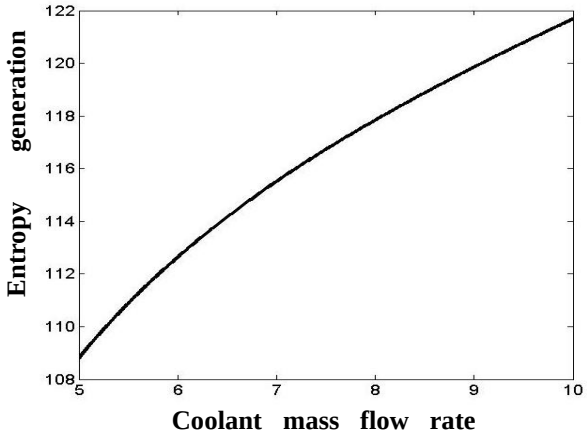

Figure 22: Effect of coolant mass flow rate on entropy generation

2.7. Results for wavy fin Radiator:

For enhancing heat transfer rate, wavy fin geometry has been used. As shown in Figs.23-27, the parametric variations are similar to louvered fin. As discussed earlier for the louvered fin geometry that with the variation of inlet air mass flow rate (Fig.23), cooling capacity increases. In the similar manner, cooling capacity, pressure drop (Fig. 24) increases with increase in coolant mass flow rate keeping other factors as a constant. On increasing inlet air temperature, the reduction in cooling capacity of radiator is observed (Fig.25) while the cooling capacity increases with the increase in coolant inlet temperature (Fig.26). And on increasing in mass flow rate of coolant, the entropy generation increases (Fig.27).

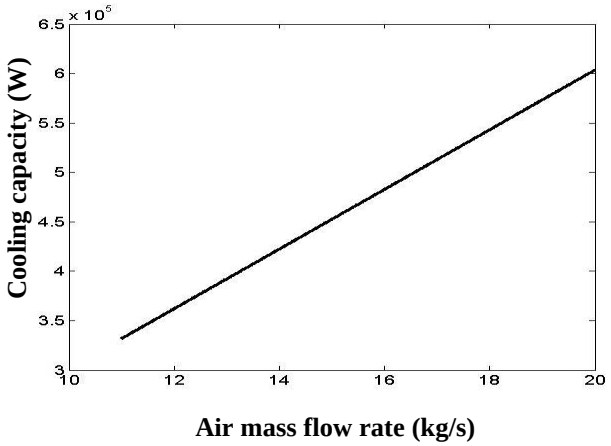

Figure 23. Effect of mass flow rate of air on cooling capacity

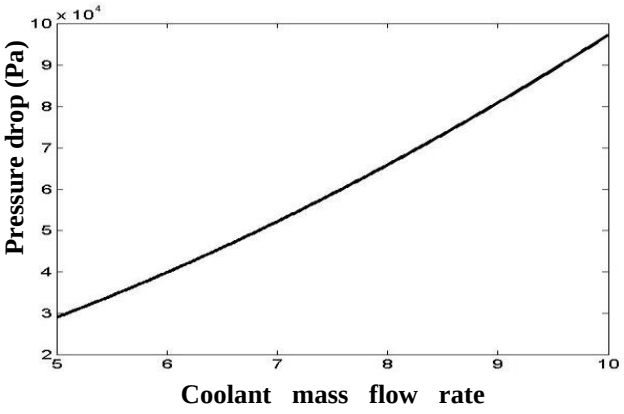

Figure 24: Effect of mass flow rate of coolant on pressure drop

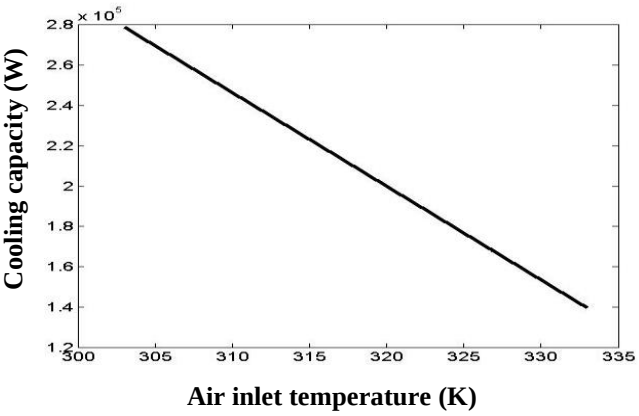

Figure 25: Effect of air inlet temperature on cooling capacitv

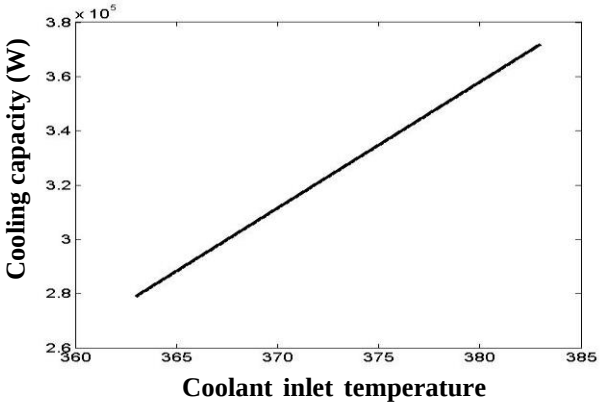

Figure 26: Effect of coolant inlet temperature on cooling capacity

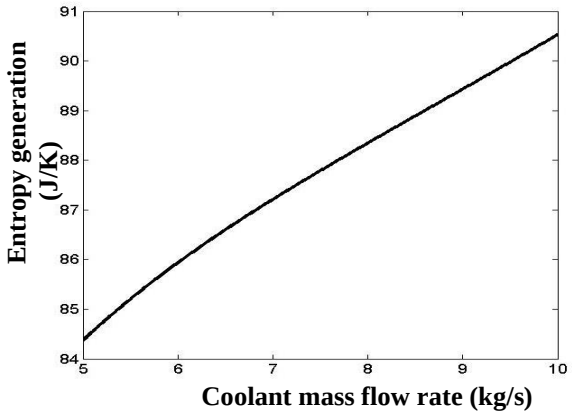

Figure 27: Effect of coolant mass flow rate on entropy generation

3.Conclusion

Heat transfer and entropy generation is determined numerically on the basis of constant heat flux and constant wall temperature condition of the tube.

Based on results and discussion, following conclusion can be made.

- In constant wall temperature, heat transfer initially increases and then decreases with respect to fin height.
- Pressure drop and friction factor always increases with fin height
- In constant wall temperature entropy generation initially increases and then decreases with fin height.
- In constant heat flux entropy generation always decreases with fin height increases.
- Nusselt number, heat transfer coefficient, Colburn factor and friction factor always increase with fin height in both the condition.

In case of constant wall temperature optimised condition is obtained. At fin height 0.002538m the heat transfer is maximum and entropy generation is neither minimum and nor maximum it lies in between.

A detailed parametric studies on automotive radiator has been done by using ε –NTU method using a base fluid 80%water-20%EG as a coolant for plate fin, louvered fin and wavy fin geometries. Detailed flow chart of the numerical method and correlations used for base fluid are presented.

- Cooling capacity and effectiveness increase with increase in mass flow rate of air and coolant.
- Cooling capacity of radiator increases with increase of coolant inlet temperature.
- Cooling capacity decreases with increase of air inlet temperature.
- Entropy generation increases with increase of both mass flow rate of air and mass flow rate of coolant.

References

1. Abbassi H. et al. (2007) *Entropy generation analysis in a uniformly heated tube heat sink. Energy, 32, 1932–47.*
2. Ahmet Z. Sahin and Rached Ben-Mansour.,(2003).*Entropy generation in laminar fluid flow through circular pipes. ISSN 1099-4300, Entropy*
3. Aroulanandam, V.V., Latchoumi, T.P., Bhavya, B., Sultana, S.S. (2019). Object detection in convolution neural networks using iterative refinements. Revue d'Intelligence Artificielle, Vol. 33, No. 5, pp. 367-372. https://doi.org/10.18280/ria.330506
4. Balamurugan, K., Uthayakumar, M., Ramakrishna, M. and Pillai, U.T.S., 2020. Air jet Erosion studies on mg/SiC composite. Silicon, 12(2), pp.413-423.
5. Balamurugan, K., 2020. Compressive Property Examination on Poly Lactic Acid-Copper Composite Filament in Fused Deposition Model–A Green Manufacturing Process. Journal of Green Engineering, 10, pp.843-852.
6. Bejan, A. (1979) *A Study of Entropy Generation in Fundamental Convective Heat Transfer," Journal of Heat Transfer, Vol. 101, pp. 718–725.*
7. Bhasha, A.C. and Balamurugan, K., 2020, July. Multi-objective optimization of high-speed end milling on Al6061/3% RHA/6% TiC reinforced hybrid composite using Taguchi coupled GRA. In 2020 International Conference on Computational Intelligence for Smart Power System and Sustainable Energy (CISPSSE) (pp. 1-6). IEEE.
8. Chang, Y. J and Wang, C. C. (1997) *A generalized heat transfer correlation for Louver fingeometry, International journal of heat transfer, 40(3) 533-544.*
9. Chinnamahammad Bhasha, A., Balamurugan, K. Fabrication and property evaluation of Al 6061 + x% (RHA + TiC) hybrid metal matrix composite. SN Appl. Sci. **1,** 977 (2019). https://doi.org/10.1007/s42452-019-1016-0
10. Demirel, Y., Kahraman, R (1999) *Entropy generation in a rectangular packed duct with wall heat flux, Int. J. Heat Mass Transfer 42, 2337–2344.*
11. Garikipati P., Balamurugan K. (2021) Abrasive Water Jet Machining Studies on $AlSi_7$+63%SiC Hybrid Composite. In: Arockiarajan A., Duraiselvam M., Raju R. (eds) Advances in Industrial Automation and Smart Manufacturing. Lecture Notes in Mechanical Engineering. Springer, Singapore. https://doi.org/10.1007/978-981-15-4739-3_66
12. Gowthaman, S., Balamurugan, K., Kumar, P.M., Ali, S.A., Kumar, K.M. and Gopal, N.V.R., 2018. Electrical discharge machining studies on monel-super alloy. Procedia Manufacturing, 20, pp.386-391.
13. Jensen, M.K.,A. Vlakancic(1999) *Experimental investigation of turbulent heat transfer and fluid flow in internally finned tubes", Int. J. Heat Mass Transfer 42, pp.1343–1351.*

14. Leong, K. Y., Saidur, R. , Kazi, S. N., Mamun, A. H. (2010) *Performance investigation of an automotive car radiator operated with nanofluid-based coolants (nanofluid as a coolant in a radiator), Applied Thermal Engineering 30, pp.2685–2692.*

15. Leong, K. Y. , Saidur, R., Kazi, S. N. , Mamun, A. H. (2010) *Performance investigation of anautomotive car radiator operated with nanofluid-based coolants (nanofluid as a coolant in aradiator), Applied Thermal Engineering 30, 2685–2692.*

16. McClintock, F. A (1951)*The Design of Heat Exchangers for Minimum Irreversibility," ASME Paper 51-A-108.*

17. Naterer, G.F., Camberos, J.A (2008) *Entropy-based Design and Analysis of Fluids Engineering Systems". CRC Press, Boca Raton.*

18. Oliet, C. , Oliva, A., Castro, J., Pe´rezSegarra. C.D.,(2007).*parametric studies on automotive radiator. Applied Thermal Engineering.*

19. Peyghambarh, S.M., Hashemabadi, S.H. , Hoseini, S.M., SeifiJamnani. M.,(2011) *Experimental study of heat transfer Enhancement using water/ethylene Glycol based nanofluids as a new Coolant for car radiators.*

20. Peyghambarzadeh , S. M., Hashemabadi , S. H. , Hoseini , S. M., SeifiJamnani, M. (2011) *Experimental study of heat transfer enhancement using water/ethylene glycol basednanofluids as a new coolant for car radiators, International communication of Heat and Masstransfer ,Article in press*

21. Ranjeeth, S., Latchoumi, T.P., Sivaram, M., Jayanthiladevi, A. and Kumar, T.S., 2019, December. Predicting Student Performance with ANNQ3H: A Case Study in Secondary Education. In 2019 International Conference on Computational Intelligence and Knowledge Economy (ICCIKE) (pp. 603-607). IEEE.

22. Webb, R.L. (1982) *Performance, cost effectiveness, and water-side fouling considerations of enhanced tube heat exchangers for boiling service with tube-side water flow", Heat Transfer Eng. 3, pp.84–98.*

23. Webb, R.L., Narayanamurthy, R., Thors, P. (2000) *Heat transfer and friction characteristics of internal helical-rib roughness", Trans. ASME: J. Heat Transfer 122, pp.134–142.*

24. Yookesh, T.L., Boobalan, E.D. and Latchoumi, T.P., 2020, March. Variational Iteration Method to Deal with Time Delay Differential Equations under Uncertainty Conditions. In 2020 International Conference on Emerging Smart Computing and Informatics (ESCI) (pp. 252-256). IEEE.

25. Zdaniuk, G.J.,. Chamra, L.M, Mago, P.J. (2008) *Experimental determination of heat transfer and friction in helically-finned tubes", Exp. Therm. Fluid Sci., submitted for publication. 32(3), 761-775.*

26. Zdaniuk, G.J., Chamra, L.M (2007) *A literature review of friction and heattransfer in helically-ribbed tubes", J. Enhanced Heat Transfer, submitted for publication.*